

See discussions, stats, and author profiles for this publication at: <https://www.researchgate.net/publication/231538439>

Density, Viscosity, and Thermal Conductivity of Electronic Grade Phosphoric Acid

ARTICLE *in* JOURNAL OF CHEMICAL & ENGINEERING DATA · DECEMBER 2010

Impact Factor: 2.04 · DOI: 10.1021/je100938j

CITATIONS

7

READS

251

5 AUTHORS, INCLUDING:



Xiaobin Jiang

Dalian University of Technology

22 PUBLICATIONS 104 CITATIONS

[SEE PROFILE](#)

Density, Viscosity, and Thermal Conductivity of Electronic Grade Phosphoric Acid

Xiaobin Jiang, Yingying Zhao, Baohong Hou,* Meijing Zhang, and Ying Bao

School of Chemical Engineering and Technology, State Key Laboratory of Chemical Engineering, Tianjin University, Tianjin 300072, People's Republic of China

The densities and viscosities of electronic grade phosphoric acid (EGPA) aqueous solutions with the mass fraction of H_3PO_4 in the range of (78.7 to 90.2) % and temperatures from (283.15 to 313.15) K were measured. The densities range from (1.606 to 1.758) $\text{g}\cdot\text{cm}^{-3}$ with the mass fraction in the range of (78.7 to 90.2) % under experimental temperature. The viscosities range from (14.63 to 134.56) $\text{mPa}\cdot\text{s}$ with the mass fraction in the range of (78.7 to 90.2) % under experimental temperature. It is found that the measured densities and viscosities are well-correlated with the temperature and mass fraction of H_3PO_4 and are fitted to the regression equations. The thermal conductivities of EGPA coarse crystal (mixture of $\text{H}_3\text{PO}_4\cdot 0.5\text{H}_2\text{O}$ crystal and phosphoric acid aqueous solution) with the initial mass fraction of H_3PO_4 in the range of (84.2 to 90) % and temperatures from (280.15 to 298.15) K were measured by the cooling rate of $2 \text{ K}\cdot\text{h}^{-1}$ with a total cooling of (3 to 4) K under the initial temperature, which simulated the operation curve in industrial application. The result shows that the thermal conductivity under this condition increases obviously when the temperature rises. The thermal conductivity decreases when the initial mass fraction of H_3PO_4 increases.

Introduction

Electronic grade phosphoric acid (EGPA) has been widely used as a high-purity chemical in the electronics industry and is mainly used for wet cleaning and wet chip etching. EGPA has an exceptionally rigorous application for impurity ion concentration. The maximum of sum impurity ion concentration is less than $1.5 \text{ mg}\cdot\text{L}^{-1}$.

A few literature studies reported the densities and viscosities of phosphoric acid. Sklyarenko and Smirnov measured the densities and viscosities of phosphoric acid in the range of (0.28 to 87.2) % in mole fraction and temperatures at (298.15, 308.15, 315.15, 323.15, and 348.15) K.¹ In the article of MacDonald and Boyack, density and specific conductivity for H_3PO_4 in the mass concentration range (86 to 102) % (the example is a mixture of orthophosphoric acid and pyrophosphoric acid when the mass fraction exceed 100 %) and temperatures at (298.15, 403.15, 413.15, 423.15, and 433.15) K were presented.² In the article of Edwards and Huffman, viscosities of phosphoric acid solutions in the concentration range (0.21 to 6.93, 9.89 to 84.77) % in mole fraction at 298.15 K were presented.³ However, few studies reported the densities and viscosities of phosphoric acid from (283.15 to 313.15) K.

Crystallization is considered as an efficient purification method for preparing EGPA. Cooling crystallization and melt crystallization were mainly researched.^{4,5} The operating temperature range for both kinds of crystallization is (285 to 310) K. The concentration of EGPA material and product is in the range (80 to 90) %. The properties of EGPA will be different with chemically pure phosphoric acid because of EGPA's relatively lower effect of impurities.⁶ So, it is necessary to measure the densities and viscosities of EGPA in the range of (78.7 to 90.2) % and temperatures from (283.15 to 313.15) K.

During the EGPA cooling crystallization process, there is a distinct coarse crystal layer attaching onto the heat transfer surface of the crystallizer, which weakens the heat transfer capacity of the equipment. In the EGPA melt crystallization process, a coarse crystal layer is generated to purify the material. So, the measurement of thermal conductivity has important significance for crystallizer design and crystallization operation. A few literature studies reported the thermal conductivity of a mixture of H_3PO_4 and H_2O or pure H_3PO_4 , which were all liquid-phase systems. Turnbull reported the thermal conductivity of phosphoric acid in two literature sources: one reported the thermal conductivity in the concentration 87 % and temperatures from (293.15 to 403.15) K,⁷ and the other one reported the thermal conductivity in the range (0 to 100) % at 298.15 K.⁸ Basil and Zachary reported the thermal conductivity in the range (84 to 115) % (the example is a mixture of orthophosphoric acid, pyrophosphoric acid, and triphosphoric acid when the mass fraction exceed 100 %) and temperatures from (298.15 to 423.15) K.⁹ However, few measured data have been reported on EGPA coarse crystal (mixture of $\text{H}_3\text{PO}_4\cdot 0.5\text{H}_2\text{O}$ crystal and phosphoric acid aqueous solution), which has a close relationship with the industrial manufacturing process.

This paper reports experimental data on densities and viscosities of EGPA aqueous solution with the mass fraction of H_3PO_4 in the range of (78.7 to 90.2) % and temperatures from (283.15 to 313.15) K. This paper also reports experimental data on thermal conductivity of EGPA coarse crystal (mixture of $\text{H}_3\text{PO}_4\cdot 0.5\text{H}_2\text{O}$ crystal and phosphoric acid aqueous solution) with the mass fraction of H_3PO_4 in the range of (84.2 to 90) % and temperatures from (280.15 to 298.15) K at atmospheric pressure. The data reported in this paper will be compared with the former literature. The EGPA coarse crystal will be discussed as a solid–liquid multiphase system and porous media filled with liquid.

* Corresponding author. Fax: +86-22-27374971. E-mail: houbaohong@tju.edu.cn.

Experimental Section

Materials. EGPA (mixture of H₃PO₄ and water, the H₃PO₄ mass fraction 90.2%, sum impurity ion concentration less than 1.2 mg·L⁻¹) was prepared by crystallization and analyzed by inductively coupled plasma-atomic emission spectrometry (ICP-AES). Ultrapure water (sum impurity ion concentration less than 0.084 mg·L⁻¹) was purified by UPW-20N ultra pure water device purchased from Beijing EPOCH Electronics Instrument Company. EGPA was diluted by ultrapure water to obtain the different mass fraction EGPA aqueous solution sample.

Apparatus and Procedures. Density and Viscosity. The mass fraction of H₃PO₄ in EGPA aqueous solution sample was determined by volumetric titration with NaOH using bromocresol green and phenolphthalein indicators with an uncertainty of (± 0.2) % in mass fraction. The density was measured with Ostwald-Sprenge type pycnometers with a bulb volume of 10 cm³ and an internal capillary diameter of about 1 mm. The internal volumes of the pycnometers were calibrated with ultrapure water at each of the experimental temperatures. The completely cleaned and dried empty pycnometers were first weighed by an electronic balance (type AB204-N, Mettler Toledo Corps) with the precision of ± 0.1 mg. Then the pycnometers filled with the experimental liquid were immersed in a water bath with a temperature stability of (± 0.05) K. The temperature of the water bath was kept at the required constant temperature for at least 2 h; the pycnometers were removed from the water bath and properly cleaned, dried, and weighed. The density was then calculated from the mass of the sample and the volume of the pycnometers. The density was averaged from the three calculated results. The absolute uncertainty of the density measurements was estimated to be within 0.002 g·cm⁻³.

The viscosity was measured by using an Ubbelohde viscometer (type 1834A, Shanghai Glass Instruments Factory, China) of (0.85, 0.95, and 1.05) mm in diameter, calibrated with ultrapure water at (283.15, 288.15, 293.15, 298.15, 303.15, 308.15, and 313.15) K. A completely cleaned and dried viscometer, filled with the experimental EGPA aqueous solution, was placed vertically in a water bath where temperature was maintained at the required constant by circulating water. After 1 h when thermal stability was attained, the flow time of the liquids was recorded with an electronic digital stop watch (± 0.01 s). Reported values in this paper were the means of at least three replicates. The viscosity of the liquids was calculated by the equation

$$\frac{\eta}{\eta_w} = \frac{\rho t}{\rho_w t_w} \quad (1)$$

where η , ρ , t , η_w , ρ_w , and t_w are the viscosity, density, and flow time of the EGPA sample and ultrapure water, respectively. The values of the viscosity and density of ultrapure water came from the literature.¹⁰ The uncertainty of viscosity measurements was within 0.28 mPa·s.

Thermal Conductivity. The basic principle of measuring thermal conductivity is the Fourier heat conduction law

$$\vec{q} = -\lambda \text{grad}t = -\lambda \frac{\partial t}{\partial n} \vec{n} \quad (2)$$

where \vec{q} , λ , gradt, ($\partial t/\partial n$), and \vec{n} are heat flux density, thermal conductivity, temperature gradient, total differential of temperature in space coordinates, and isothermal surface normal vector.

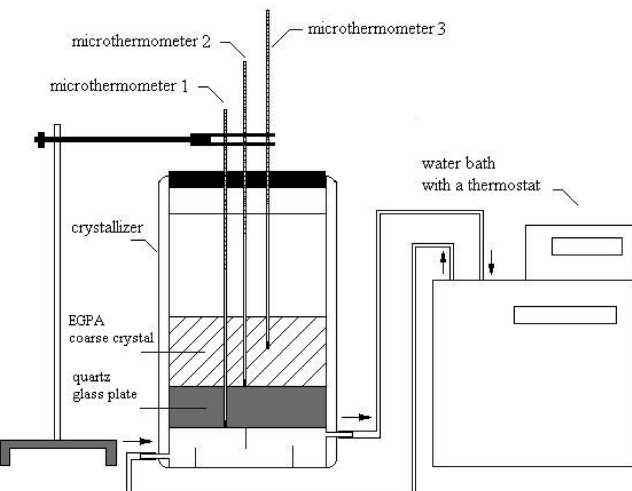


Figure 1. Schematic diagram of the experimental apparatus for measuring the thermal conductivity of EGPA coarse crystal.

In cylindrical coordinates, the isothermal surface parallels the bottom of the cylinder if the surface heat source is the bottom of the cylinder and the sidewall of cylinder is well-insulated. On these premises, the Fourier equation can be written in one-dimensional static form

$$\vec{q}_x = -\lambda \frac{dt}{dx} \vec{i} \quad (3)$$

where \vec{i} is the one-dimensional heat flux direction vector of the x -axis. It is assumed that the temperature gradient remains constant at a certain distance [(1 to 2) cm in the x -axis, compared to the radius of the isothermal surface, 15 cm]. So, eq 3 can be transformed into

$$\vec{q}_x = -\lambda \frac{\Delta t}{\Delta x} \vec{i} \quad (4)$$

where Δx and Δt are the vertical distance of the two interfaces of crystal layer and the temperature difference between the two interfaces.¹¹

The longitudinal heat flow method was used in this paper. The test sample was placed on the known thermal conductivity and thickness reference object. Under the assumption that the heat flow rate through the test sample was the same as the one through the reference object, the thermal conductivity could be derived by the following equations

$$\vec{q}_x = -\lambda_{\text{test}} \frac{\Delta t_{\text{test}}}{\Delta x_{\text{test}}} \vec{i} = -\lambda_{\text{ref}} \frac{\Delta t_{\text{ref}}}{\Delta x_{\text{ref}}} \vec{i} \quad (5)$$

$$\lambda_{\text{test}} = \lambda_{\text{ref}} \frac{\left(\frac{\Delta t_{\text{ref}}}{\Delta x_{\text{ref}}} \right)}{\left(\frac{\Delta t_{\text{test}}}{\Delta x_{\text{test}}} \right)} \quad (6)$$

where the subscript test and ref are the test sample and reference object.

The thermal conductivity was measured by the apparatus shown in Figure 1. The crystallizer (inner diameter 30 cm, height

Table 1. Viscosity η and Density ρ for EGPA from $T = (283.15$ to $313.15)$ K as a Function of Mass Fraction of w of H_3PO_4

$100 w$	T K	ρ $\text{g}\cdot\text{cm}^{-3}$	η $\text{mPa}\cdot\text{s}$	$100(\eta_{\text{exp}} - \eta_{\text{cal}})/\eta_{\text{exp}}$	$100 w$	T K	ρ $\text{g}\cdot\text{cm}^{-3}$	η $\text{mPa}\cdot\text{s}$	$100(\eta_{\text{exp}} - \eta_{\text{cal}})/\eta_{\text{exp}}$
78.7	283.15	1.622	38.59	4.38	88.0	283.15	1.733	104.82	3.55
	288.15	1.619	32.40	2.51		288.15	1.730	79.65	-1.35
	293.15	1.617	27.70	2.42		293.15	1.726	64.47	0.04
	298.15	1.615	24.33	4.92		298.15	1.722	50.35	-2.20
	303.15	1.611	20.30	2.48		303.15	1.718	38.68	-6.21
	308.15	1.608	17.53	3.33		308.15	1.714	31.89	-2.84
	313.15	1.606	14.63	0.88		313.15	1.710	25.30	-3.52
	283.15	1.652	51.23	6.40		283.15	1.748	116.13	1.58
	288.15	1.649	40.53	0.56		288.15	1.744	91.74	1.37
	293.15	1.645	32.01	-5.84		293.15	1.739	69.15	-3.59
81.1	298.15	1.643	27.61	-3.13	89.2	298.15	1.736	54.12	-4.79
	303.15	1.637	23.66	-1.14		303.15	1.733	43.03	-4.36
	308.15	1.632	19.85	-1.33		308.15	1.728	33.90	-4.87
	313.15	1.629	17.70	4.47		313.15	1.724	27.25	-3.27
	283.15	1.693	67.60	-4.19		283.15	1.753	125.36	3.69
	288.15	1.689	53.85	-7.07		288.15	1.749	96.58	1.40
84.7	293.15	1.685	46.83	-0.77	89.7	293.15	1.745	75.28	0.23
	298.15	1.683	37.59	-2.76		298.15	1.742	60.30	1.76
	303.15	1.681	30.35	-4.18		303.15	1.738	46.81	0.20
	308.15	1.676	24.19	-7.01		308.15	1.733	37.64	2.09
	313.15	1.670	21.48	1.39		313.15	1.729	29.46	1.34
	283.15	1.712	84.35	0.68		283.15	1.758	134.56	6.96
86.3	288.15	1.709	63.91	-6.02	90.1	288.15	1.754	100.26	1.80
	293.15	1.705	54.26	-1.01		293.15	1.751	79.20	2.17
	298.15	1.703	43.17	-2.68		298.15	1.747	64.75	5.89
	303.15	1.698	34.61	-3.59		303.15	1.743	52.57	8.82
	308.15	1.695	27.64	-4.94		308.15	1.739	41.08	8.21
	313.15	1.693	22.64	-3.59		313.15	1.734	32.10	7.62

55 cm) had a jacket in bottom for water circulating, a jacket filled with air around its bottle, and a plug on the top to keep the crystallizer well-insulated. The quartz glass as the reference object with a known thickness was placed at the bottom of the crystallizer. Three microthermometers (± 0.05 K) were located to determine the temperature of the corresponding interface. The thickness of the coarse crystal layer was determined by measuring the vertical distance between the second and third microthermometer's bottom using a vernier caliper (± 0.05 mm). A certain amount of EGPA aqueous solution (about 1000 g) with a known H_3PO_4 mass fraction was added into the crystallizer. A bit of EGPA crystal (about 0.1 g) as crystal seed was added into the crystallizer 1 h later when the material temperature was kept at the saturation temperature of EGPA aqueous solution. The EGPA aqueous solution was cooled by circulating water of the crystallizer bottom jacket, and $\text{H}_3\text{PO}_4 \cdot 0.5\text{H}_2\text{O}$ crystal grew homogeneously from bottom; thus, the system is a mixture of $\text{H}_3\text{PO}_4 \cdot 0.5\text{H}_2\text{O}$ crystal and phosphoric acid aqueous solution, that is, EGPA coarse crystal. The EGPA solution material was slowly cooled in the cooling rate of 2 K per hour (consistent with industrial process) until its temperature was (3 to 4) K lower than the initial value. When the coarse crystal had grown to the certain thickness which had covered microthermometer's bottom, the temperature values of three microthermometers were recorded every 15 min. When temperature values of the third microthermometer were kept invariant (the variation smaller than ± 0.05 K) for more than 1 h, it was considered that the crystallization came to a dynamic equilibrium, and the effect of crystallization enthalpy and mixing heat on thermal conductivity measurement can be neglected. Then we cooled the circulating water with the same cooling rate to a lower temperature (about 2 K lower) and repeated the above procedure until the set temperature was 280 K. The uncertainty of thermal conductivity measurements was within $0.02 \text{ W}\cdot\text{m}^{-1}\cdot\text{K}^{-1}$.

Results and Discussion

Density and Viscosity. The experimental densities of EGPA aqueous solution measured for all experimental mass fractions and different temperatures are listed in Table 1. The viscosities of EGPA aqueous solution calculated from eq 1 for all experimental mass fractions and different temperatures are listed in Table 1 and presented in Figure 2 [viscosity η vs temperature t from (283.15 to 313.15) K and mass fraction w from (78.5 to 90.5) %].

The viscosity η can be fitted by the least-squares method as the following equation

$$\ln(\eta/\text{mPa}\cdot\text{s}) = aw + b \quad (7)$$

where w is the H_3PO_4 mass fraction and a and b are coefficients. The values of coefficients a and b calculated from eq 7 are listed

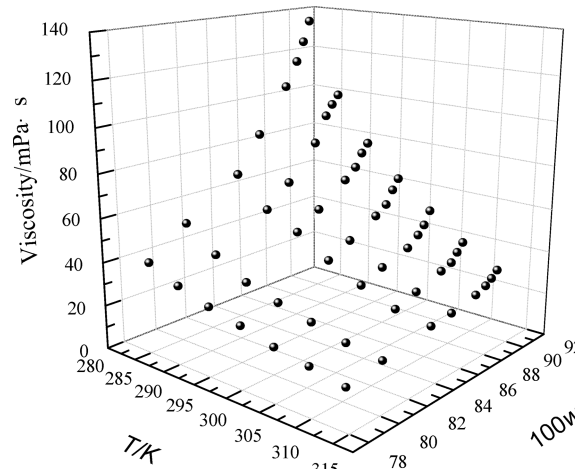


Figure 2. Viscosity η vs temperature T from (283.15 to 313.15) K and mass fraction w from (78.5 to 90.5) %.

Table 2. Coefficients a and b and Average Relative Deviations (%ARDs) for Equation 7 from $T = (283.15$ to $313.15)$ K

coef. in eq 7	T/K						
	283.15	288.15	293.15	298.15	303.15	308.15	313.15
a	0.1072	0.1002	0.0935	0.0848	0.0783	0.0714	0.0622
b	-4.7913	-4.4420	-4.0758	-3.5309	-3.1837	-2.8039	-2.2051
%ARD	0.60	0.71	0.52	0.93	1.00	1.22	0.96

in Table 2. The effects of temperature on coefficients a and b can be seen from Figure 3. The dependence of the coefficients a and b in eq 7 on the temperature can be described by the following equations

$$a = k_a \exp(l_a(T - 273.15)/K) \quad (8)$$

$$a = m_a(T - 273.15)/K + n_a \quad (9)$$

$$b = k_b \exp(l_b(T - 273.15)/K) \quad (10)$$

$$b = m_b(T - 273.15)/K + n_b \quad (11)$$

where t is temperature and k_a , l_a , m_a , n_a , k_b , l_b , m_b , and n_b are coefficients. The averaged relative deviation (ARD, computation expression shown in eq 16) of coefficients a and b at different temperatures are also listed in Table 2, and all ARDs are less than 2.0 %, which demonstrates a good fit in eq 7.

The values of the coefficients k_a , l_a , m_a , n_a , k_b , l_b , m_b , and n_b in eqs 8 to 11 for all of the multiplicate mass fractions of EGPA are listed in Table 3. It is seen from Table 3 that the ARD of eq 9 (0.72) is correspondingly smaller than that of eq 8 (1.70), which means eq 9 fits parameter a better than eq 8. Likewise, eq 11 (ARD 1.83) fits parameter b better than eq 10 (ARD 3.79).

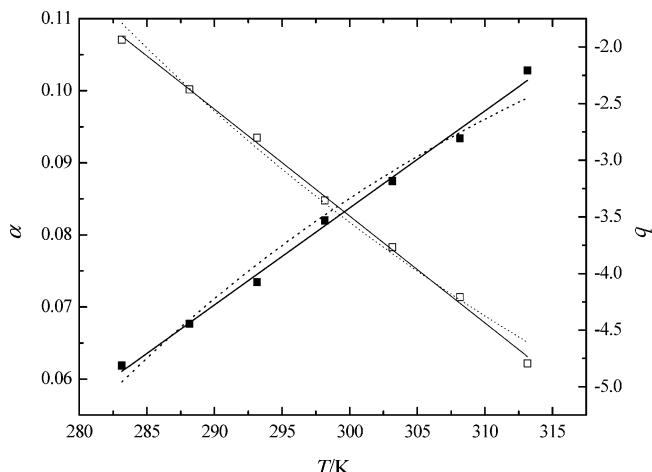


Figure 3. Coefficients a and b in eq 7 vs temperature T from (283.15 to 313.15) K. □, coefficient a ; ■, coefficient b ; —, linear regression; ..., exponential regression.

Table 3. Coefficients k_a , l_a , m_a , n_a , k_b , l_b , m_b , and n_b and ARDs for Equations 8, 9, 10, and 11

eq 8			eq 9		
k_a	l_a	ARD	m_a	n_a	ARD
-0.0178	-2.0320	1.70	-0.001485	0.1225	0.72
<hr/>					
eq 10			eq 11		
k_b	l_b	ARD	m_b	n_b	ARD
-0.0250	1.8676	3.79	0.0852	-5.7059	1.83

Therefore, the dependence of the coefficient a in eq 7 on the temperature can be described by eq 9 and the coefficient b by eq 11. So, the viscosity of EGPA can be presented by the equation

$$\ln(\eta/\text{mPa}\cdot\text{s}) = (-0.001485((T - 273.15)/\text{K}) + 0.1225)(100w) + 0.0852((T - 273.15)/\text{K}) - 5.7059 \quad (12)$$

It can be seen from Figure 2 that the viscosities of EGPA aqueous solution increase sharply with increasing mass fraction of H_3PO_4 and falling temperature, which deteriorates the diffusion and mass transfer process and increases the time and difficulty of the crystallization process.

In this paper, the densities of EGPA were used as the foundational data for viscosities measurement. In addition, the densities of EGPA were useful as basic property data of phosphoric acid. Meanwhile in literature,² the following equation was fitted to the density data they measured

$$\rho = 0.68235 + 1.20811 \cdot 10^{-2}w - (1.2379 \cdot 10^{-3} - 3.7938 \cdot 10^{-6}w)t \quad (13)$$

where ρ , w , and t are the density ($\text{g}\cdot\text{cm}^{-3}$), concentration, expressed in weight percent, and the temperature ($^{\circ}\text{C}$). Because the author measured the densities of phosphoric acid (chemical pure grade) at the temperatures (298.15, 403.15, 413.15, 423.15, 433.15) K, the equation fit better in a higher temperature range (higher than 403.15 K). The density data measured in literature² and in this paper were shown in Figure 4 to make a comparison, and both of them had good consistency. However, the density data measured for industry application temperature range (283.15 to 313.15) K were not enough and had lower precision

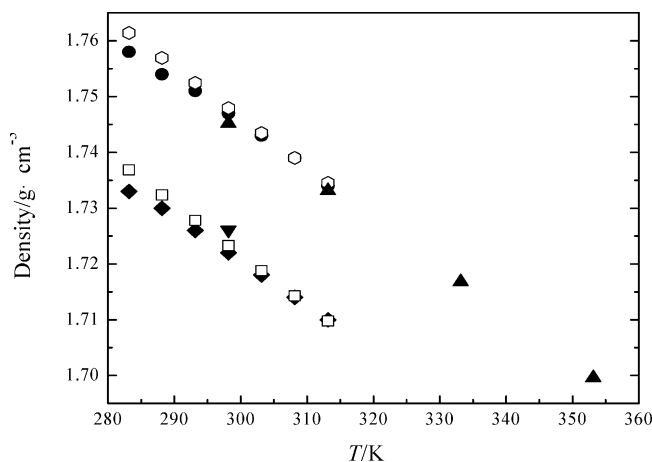


Figure 4. Density data comparison with literature.² Data in this paper: ◆, 88.0 %, (283.15 to 313.15) K; ●, 90.1 %, (283.15 to 313.15) K. Data calculated by eq 13: □, 88.0 %, (283.15 to 313.15) K; ○, 90.1 %, (283.15 to 313.15) K. Data in literature 2: ▼, 88.28 %, 298.15 K; ▲, 90 %, (298.15 to 353.15) K.

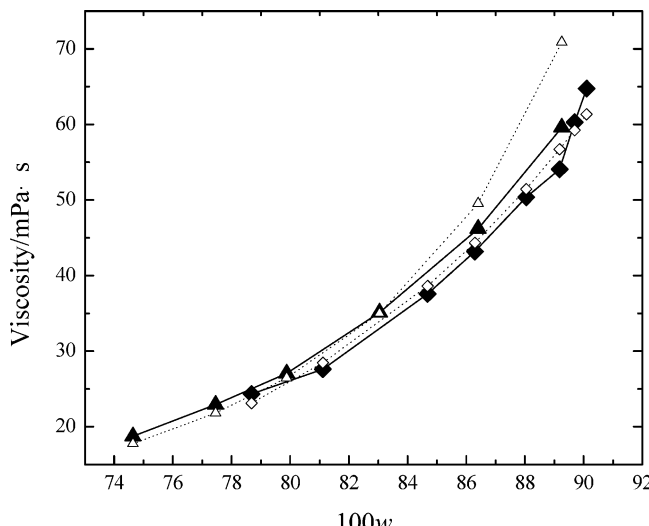


Figure 5. Viscosity data (298.15 K) comparison with literature³ and eq 14. Data in this paper: ♦, measured data; ◇, data calculated by eq 12. Data in literature 3: ▲, measured data; △, data calculated by eq 14.

in literature.² Density data in this paper were measured in detail at the temperature range (283.15 to 313.15) K and had a higher precision.

In literature,³ the author measured the viscosities of phosphoric acid at 298.15 K, and the data were fit by three different equations based on the molality of phosphoric acid. In literature,³



Figure 6. EGPA coarse crystal (mixture of $\text{H}_3\text{PO}_4 \cdot 0.5\text{H}_2\text{O}$ crystal and phosphoric acid aqueous solution).

the following equation covered the concentration range of that paper ($m = 9.89$ to 50, namely, $w = 49.2\%$ to 89.2%)

$$\log(\eta/\text{mPa}\cdot\text{s} - 0.8902) = 1.334646 \log m - 0.723152 \quad (14)$$

The viscosity data measured in literature³ and in this paper were shown in Figure 5 (the parameter transformation was done, and the abscissa was uniformed to w , mass fraction), and a comparison of the fitting results expressed by eqs 12 and 14 was also shown. It is seen that the viscosity data in literature³ are on average 5 % higher than that in this paper, which may

Table 4. Thermal Conductivity λ for EGPA Coarse Crystal at Atmospheric Pressure as a Function of Temperature

100 w_1	T K	λ $\text{W}\cdot\text{m}^{-1}\cdot\text{K}^{-1}$	$100(\lambda_{\text{exp}} - \lambda_{\text{cal}})/\lambda_{\text{exp}}$	100 w_1	T K	λ $\text{W}\cdot\text{m}^{-1}\cdot\text{K}^{-1}$	$100(\lambda_{\text{exp}} - \lambda_{\text{cal}})/\lambda_{\text{exp}}$
84.2	290.60	0.313	1.41	87.7	297.10	0.411	0.00
	289.60	0.272	-2.48		296.70	0.388	-0.90
	287.60	0.241	0.02		295.60	0.346	-0.54
	286.75	0.238	2.28		295.05	0.324	-2.00
	284.25	0.221	-0.91		293.00	0.299	3.08
	281.95	0.216	-0.43		290.95	0.274	0.55
	280.75	0.208	0.22		288.40	0.257	-2.28
	280.40	0.204	0.25		286.45	0.249	1.08
	292.20	0.335	1.00		297.55	0.417	-1.20
	291.55	0.309	-1.40		296.70	0.389	2.73
85.5	290.20	0.285	-0.70	88.7	295.65	0.333	-1.33
	288.30	0.269	0.65		294.45	0.298	-2.21
	286.30	0.262	1.37		292.45	0.280	2.18
	284.40	0.245	-1.69		289.90	0.257	-0.71
	283.30	0.237	-1.12		288.20	0.250	-0.29
	282.65	0.234	1.40		286.85	0.238	0.22
	292.80	0.347	0.40		298.15	0.429	1.64
	292.30	0.332	0.05		297.70	0.390	-1.89
	289.95	0.285	-0.98		296.65	0.343	-0.99
	288.70	0.280	0.98		295.15	0.297	0.01
86.8	287.15	0.271	0.51	90.0	293.10	0.267	1.30
	285.50	0.260	-0.62		290.15	0.255	0.78
	284.40	0.252	-0.50		288.60	0.244	-2.50
	283.70	0.247	0.57		286.85	0.242	1.06

Table 5. Solubility of Orthophosphoric Acid in Water (Solid Phase: $\text{H}_3\text{PO}_4 \cdot 0.5\text{H}_2\text{O}$) and the Mass Fraction of $\text{H}_3\text{PO}_4 \cdot 0.5\text{H}_2\text{O}$ with Different w_{initial}

T/K	mass of H_3PO_4 per 100 g of satd. soln., g	mass fraction of $\text{H}_3\text{PO}_4 \cdot 0.5\text{H}_2\text{O}$, %				
		$w_{\text{initial}}, 84.2$	$w_{\text{initial}}, 85.5$	$w_{\text{initial}}, 86.8$	$w_{\text{initial}}, 87.7$	$w_{\text{initial}}, 88.7$
273.15	78.75	45.83	56.96	68.09	75.80	84.36
292.07	84.07		26.56	44.17	56.36	69.90
296.56	85.93			15.10	32.74	52.34
298.39	87.05				10.52	35.82
300.45	88.51					44.92
301.90	90.00					0

Table 6. Coefficients A_0 , A_1 , A_2 , and A_3 and Average Relative Deviations (ARDs) for Equation 15

coef. in eq 15	84.2	85.5	86.8	87.7	88.7	90.0
A_0	-0.1607	-0.4494	-0.5653	-1.1070	-1.1849	-1.287
$10A_1$	1.0175	1.5310	1.7229	2.3951	2.5091	2.7155
$100A_2$	-0.9128	-1.1265	-1.2115	-1.4152	-1.4761	-1.6003
$1000A_3$	0.2774	0.2824	0.2906	0.2838	0.2941	0.3151
ARD	1.02	1.17	0.58	1.42	1.36	1.27

be the impurity effect (phosphoric acid measured in literature³ was purified chemical pure grade). In addition, eq 12 fitted the viscosity data measured in this paper well in the overall range of concentration, while eq 14 had a significant error when w was above 86 %. Besides, eq 14 was only applied to 298.15 K. The phosphoric acids with mass fractions from 80 % to 90 % were mainly used in industry crystallization, so the viscosity data in this concentration interval was very important.

To sum up, the data in Table 1 and eq 12 are considered to be widely applicable and reliable.

Thermal Conductivity. The thermal conductivities of EGPA coarse crystal calculated from eq 6 for all experimental samples at different temperatures are listed in Table 4.

The thermal conductivity is normally associated with temperature. It is commonly known that the solid-to-liquid ratio of EGPA coarse crystal (mixture of $H_3PO_4 \cdot 0.5H_2O$ crystal and phosphoric acid aqueous solution) increases with the temperature reduction. For the different heat-conducting properties between solid and liquid EGPA, the thermal conductivity varies not only with the temperature but also with the solid-to-liquid ratio. Literature¹² reported the solubility of orthophosphocia acid (solid phase $H_3PO_4 \cdot 0.5H_2O$); the data are shown in Table 5. The mass fractions of $H_3PO_4 \cdot 0.5H_2O$ with different $w_{initial}$ at the corresponding temperature are also listed in Table 5. It is indicated that, in the temperature range (280.4 to 298.15) K, the mass fraction of $H_3PO_4 \cdot 0.5H_2O$ crystal changes in a large range. The cooling process was carried out very slowly ($2\text{ K} \cdot \text{h}^{-1}$), with quite an amount of aqueous liquid still mixed within the crystal (shown in Figure 6), that is, coarse crystal. In addition, $H_3PO_4 \cdot 0.5H_2O$ crystal grown in this cooling process was inclined to be fine cuboid, which deteriorated the aqueous liquid separated from crystal phase and easily encapsulated the aqueous liquid. So, the thermal conductivities of EGPA coarse crystal (mixture of $H_3PO_4 \cdot 0.5H_2O$ crystal and phosphoric acid aqueous solution, which is considered to be a solid–liquid multiphase system) data were measured in this paper.

Meanwhile, the crystal mass fraction is associated with the initial mass fraction and temperature. Moreover, EGPA with different initial mass fractions holds a diverse crystallization operation temperature interval, which makes it very difficult to fit the thermal conductivity with the mass fraction. So, the thermal conductivity of EGPA coarse crystal can be fitted by the least-squares method as in the following equation

$$\lambda = A_0 + A_1((T - 273.15)/\text{K}) + A_2((T - 273.15)/\text{K})^2 + A_3((T - 273.15)/\text{K})^3 \quad (15)$$

where t is the average temperature of the two crystal interfaces and A_0 , A_1 , A_2 , and A_3 are coefficients. The values of coefficients A_0 , A_1 , A_2 , and A_3 calculated from eq 15 are listed in Table 6. The effects of the initial mass fraction on the coefficients A_0 , A_1 , A_2 , and A_3 can be seen from Figure 7. It is shown that the initial mass of the H_3PO_4 fraction has little effect on A_2 and A_3 but obviously on A_0 and A_1 .

The ARD of the measured data to the calculated data is defined as follows

$$\text{ARD}(x) = \frac{100}{N} \sum \frac{|x_i - x_{i(\text{cal})}|}{x_i} \quad (16)$$

where x is the measured data (η or λ) and the subscript cal represents the values calculated from eqs 12 and 15.

The average relative deviations (ARD) of eq 15 at different initial mass fractions are listed in Table 6, and all ARDs are smaller than 1.5 %, which demonstrates a good fit in eq 15.

It can be seen from Figure 8 and Table 4 that the thermal conductivities decrease markedly with the reducing temperature.

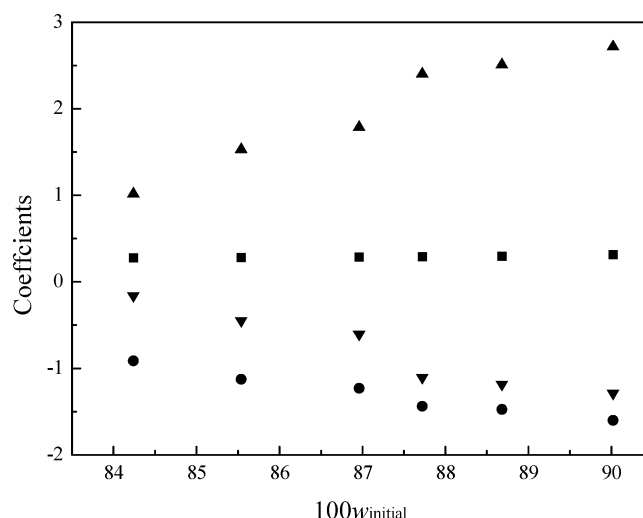


Figure 7. Coefficients A_0 , A_1 , A_2 , and A_3 in eq 15 vs initial mass fraction w from (84 to 90) %. ▼, A_0 ; ▲, $10A_1$; ■, $100A_2$; ●, $1000A_3$.

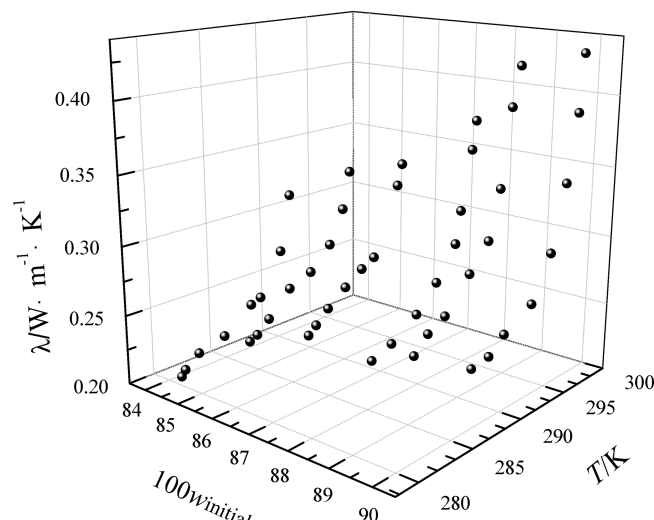


Figure 8. Thermal conductivity λ vs temperature T from (280.15 to 298.15) K and mass fraction w from (84.2 to 90.0) %.

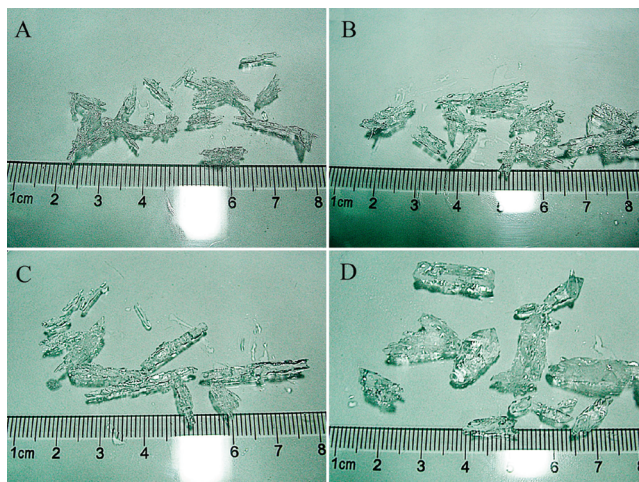


Figure 9. $\text{H}_3\text{PO}_4 \cdot 0.5\text{H}_2\text{O}$ crystal with different initial mass fractions w_{initial} : A, 85.5 %, 282.65 K; B, 86.8 %, 283.7 K; C, 88.7 %, 286.85 K; D, 90.0 %, 286.85 K.

When the temperatures are same, the thermal conductivities decrease at a certain extent with increasing the initial mass fraction of EGPA. There are two reasons.

1. As had been noted, the measured thermal conductivities were assigned to EGPA coarse crystal, a solid–liquid multiphase system. So when the temperature went down, the mass fraction of the liquid phase decreased, and the mass fraction of the crystal phase increased. Because the thermal conductivities of crystal and liquid phase were different, the thermal conductivities changed with the temperature went down.

2. EGPA coarse crystal, a solid–liquid multiphase system, was also classified into porous media (the crystal layer of $\text{H}_3\text{PO}_4 \cdot 0.5\text{H}_2\text{O}$ crystal) filled with liquid (phosphoric acid aqueous solution). As reported in literature,¹³ the proposed model-represented porous media properties were expressed as a function of tortuosity, porosity, resistance coefficient, ratio of pore diameter to throat diameter, and fluid properties.

As shown in Figure 9 (crystal grown with different initial mass fractions), $\text{H}_3\text{PO}_4 \cdot 0.5\text{H}_2\text{O}$ crystal had a different crystal habit and crystal size distribution (CSD) when the initial mass fraction was different. With a higher initial mass fraction, the crystal had a bigger size and a smoother surface. All of the variations of crystal habit and CSD will lead to the change of tortuosity, porosity, resistance coefficient, and so forth, and finally change the properties of porous media.

Considering porous media was a complex system and the model included many parameters, further research was not carried out in this paper.

The mass fractions of six experimental EGPA aqueous solutions have covered the mass fractions of common raw materials for EGPA preparation. Equation 15 can be used directly in EGPA manufacturing production within the acceptable error. Obviously the manufacturing process should be similar to the experimental condition [the cooling rate of $2 \text{ K} \cdot \text{h}^{-1}$ with a total cooling of (3 to 4) K under the initial temperature] when the data were applied. Therefore, different manufacturing conditions will produce different crystal sizes and make the effective thermal conductivity different.

Conclusion

The viscosities of EGPA aqueous solutions are obtained in the temperature range from (283.15 to 313.15) K and H_3PO_4 mass fraction (78.7 to 90.2) %, and they are found to be well-correlated with the temperature and mass fraction of H_3PO_4 . According to the results, crystallization operating with higher temperatures is more advisable for EGPA preparation.

The thermal conductivities of EGPA coarse crystal are also obtained in the temperature range from (280.15 to 298.15) K and initial H_3PO_4 mass fractions (84.4 to 90.0) %, and they are found to be well-correlated with temperature. The initial mass fraction also affects the thermal conductivities. Because the thermal conductivities of EGPA coarse crystal decrease significantly with the temperature decreases, a higher heat exchanging efficiency is an essential requirement for the crystallizer to meet operation demand at the late to mid-crystallization period of cooling or melt crystallization.

The data reported in this paper were also compared with the former literature. For the data measured with a higher purity example EGPA at a temperature and concentration range more useful for engineering applications, the data reported in this paper were widely applicable. The EGPA coarse crystal was discussed as a solid–liquid multiphase system and porous media filled with liquid. A good explanation has been made for the change in thermal conductivities with temperature and EGPA initial mass fraction.

Literature Cited

- (1) Sklyarenko, S. I.; Smirnov, I. V. Conductivity, Viscosity and Density of Aqueous Solutions of Orthophosphoric Acid. *Zh. Fiz. Khim.* **1951**, *25*, 24–28.
- (2) MacDonald, D. I.; Boyack, J. R. Density, Electrical Conductivity, and Vapor Pressure of Concentrated Phosphoric Acid. *J. Chem. Eng. Data* **1969**, *14*, 380–384.
- (3) Edwards, O. W.; Huffman, E. O. Viscosity of Aqueous Solutions of Phosphoric Acid at 25 °C. *Chem. Eng. Data Ser.* **1958**, *3*, 145.
- (4) Kim, K. J. Purification of Phosphoric Acid from Waste Acid Etchant Using Layer Melt Crystallization. *Chem. Eng. Technol.* **2006**, *29*, 271–276.
- (5) Xiao, L. H.; Zeng, B. Research Advances on Electronic Grade Phosphoric Acid. *Yunnan Chem. Technol.* **2007**, *34*, 60–63.
- (6) Cate, W. E.; Deming, M. E. Effect of Impurities on Density and Viscosity of Simulated Wet-Process Phosphoric Acid. *J. Chem. Eng. Data* **1970**, *15*, 290–295.
- (7) Turnbull, A. G. Thermal Conductivity of Phosphoric Acid. *J. Chem. Eng. Data* **1965**, *10*, 118–119.
- (8) Turnbull, A. G. Thermal Conductivity of Phosphoric Acid-Water Mixtures at 25 °C. *J. Chem. Eng. Data* **1971**, *16*, 79–83.
- (9) Luff, B. B.; Wakefield, Z. T. Thermal Conductivity of Phosphoric Acid. *J. Chem. Eng. Data* **1969**, *14*, 254–256.
- (10) Cheng, N. L.; Hu, S. W. *Solvents Handbook*, 4th ed.; Chemical Engineering Press: Beijing, 2008.
- (11) Savino, J. M.; Siegel, R. An Analytical Solution for Solidification of A Moving Warm Liquid onto an Isothermal Cold Wall. *Int. J. Heat Mass Transfer* **1969**, *12*, 803–809.
- (12) Ross, W. H.; Jones, R. M. The Solubility and Freezing-point Curves of Hydrated and Anhydrous Orthophosphoric Acid. *J. Am. Chem. Soc.* **1925**, *47*, 2165–2171.
- (13) Wu, J. S.; Yin, S. X. A Micro-mechanism Model for Porous Media. *Commun. Theor. Phys.* **2009**, *52*, 936–940.

Received for review June 17, 2010. Accepted December 27, 2010.

JE100938J